ChemPubSoc Europe

DOI: 10.1002/open.201700057

Open Access ChemistryOPEN Full Papers

Potassium-Ion-Selective Fluorescent Sensors To Detect Cereulide, the Emetic Toxin of *B. cereus*, in Food Samples and HeLa Cells

José García-Calvo,[a] Saturnino Ibeas,[a] Eva-Clara Antón-García,[a] Tomás Torroba,*[a] Gerardo González-Aguilar,[b] Wilson Antunes,[c] Eloísa González-Lavado,[d] and Mónica L. Fanarraga*[d]

This paper is dedicated to the memory of the late Dr. Stefano Marcaccini

We report the development of new chemical probes for cereulide, a toxic metabolite produced by specific strains of *Bacillus cereus*, through displacement of potassium cations from a preformed specific complex and a subsequent change in the fluorescence emission. For this purpose, we designed fluorescent probes for potassium cations that were suitable for displacement assays with cereulide from organic extracts. The fluorescence detection of natural cereulide in rice samples was achieved by using synthetic cereulide as a reference and a potassium fluorescent reporter, and this was found to be useful as a portable and fast method for the in situ detection of cereulide in food extracts. To study the fate of cereulide in live cells, we designed a procedure that was suitable for live-cell microscopy imaging of HeLa cells by comparing the cellular location of the potassium fluorogenic probe, which stained intracellular endolysosomes, in the absence and presence of cereulide; we concluded that in the presence of cereulide, the fluorescence of the probe was decreased because of complexation of the potassium ions by cereulide.

1. Introduction

Cereulide is an ionophore toxin produced by specific strains of *Bacillus cereus*.[1] *B. cereus* causes two different types of food disease: diarrheal and emetic syndrome.[2] The diarrheal form is developed after the ingestion of food contaminated with spores or vegetative cells able to produce enterotoxins during vegetative growth in the small intestine. The emetic syndrome is usually associated with the ingestion of foodstuffs contaminated with the preformed toxin, cereulide, produced during the growth of bacteria in food;[3] therefore, intoxication with cereulide could be prevented by the early detection of the toxin in food. *B. cereus* can produce highly resistant structures called endospores, which are capable of surviving to cooking temperatures. *Bacillus* endospores present in foodstuffs can rapidly germinate and produce their toxins, especially during food chilling or food heating.[4] *B. cereus* is a ubiquitous agent in nature, and their spores can be found as a natural contaminant in several food products, especially meats, vegetables, and milk.[5] The emetic syndrome is generally associated with rice or other starch-rich products such as pasta and potato-based products.[6] The emetic toxin is a cyclic depsipeptide[7] with the structure [D-*O*-Leu-D-Ala-L-*O*-Val-L-Val]$_3$, which is closely related to the structure of valinomycin, another naturally occurring cyclic depsipeptide and potassium-cation ionophore with the tetramer structure D-α-hydroxyisovaleryl-D-valyl-L-lactyl-L-valyl [D-*O*-Hyi-D-Val-L-*O*-Lac-L-Val]$_3$ (Figure 1).[8] The cer-

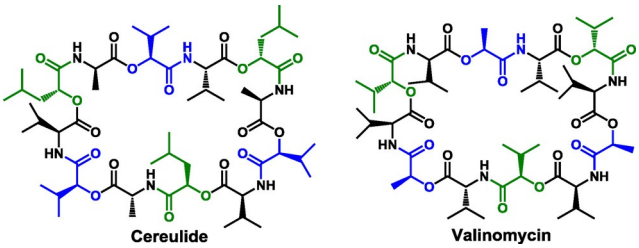

Figure 1. Chemical structures of cereulide and valinomycin.

[a] J. García-Calvo, Dr. S. Ibeas, E.-C. Antón-García, Prof. T. Torroba
Department of Chemistry, Faculty of Science
University of Burgos, 09001 Burgos (Spain)
E-mail: ttorroba@ubu.es

[b] Dr. G. González-Aguilar
Centre for Applied Photonics, INESC TEC
Rua do Campo Alegre, Dpto. Física 4169-007 Porto (Portugal)

[c] Dr. W. Antunes
Laboratório de Bromatologia e de Defesa Biológica (LBDB) do Exército
Av. Dr. Alfredo Bensaúde, 1849-012 Lisboa (Portugal)

[d] E. González-Lavado, Prof. M. L. Fanarraga
Grupo de Nanomedicina-IDIVAL
Universidad de Cantabria, Santander 39011 (Spain)
E-mail: monica.lopez@unican.es

Supporting Information and the ORCID identification number(s) for the author(s) of this article can be found under https://doi.org/10.1002/open.201700057.

eulide toxin is usually identified by liquid chromatography and mass spectrometry, which require dedicated facilities.[9] Cereulide acts as a potassium-cation ionophore and is able to disrupt the transmembrane potential in mitochondria of eukaryotic cells; this leads to mitochondrial degeneration and subsequently to cell death.[10] Owing to cereulide toxicity, rapid and portable detection methods to screen the presence of preformed toxin in foodstuffs are required to prevent the occurrence of food-borne outbreaks by emetic toxin.

2. Results and Discussion

Fluorescent probes are a good alternative for the detection of toxins or chemical threats.[11] Owing to the ability of cereulide to complex potassium cations, a suitable method for its detection from extracts of biological or food samples should be a displacement mechanism of the potassium cation from a preformed specific complex that would give rise to a change in the fluorescence emission. Following this idea, we designed a fluorescent probe for potassium that is suitable for displacement assays with cereulide in organic solvents. Because cereulide is not soluble in water, a requisite of the fluorogenic probe is that it have good performance in organic or mixed organic–aqueous solvents. Therefore, we selected a perylenemonoimide as the fluorescent reporter[12] and a K^+-selective phenylaza[18]crown-6-lariat-ether[13] or a triazacryptand[14] as the recognition units and bonded both moieties in every case by Suzuki coupling (Scheme 1).

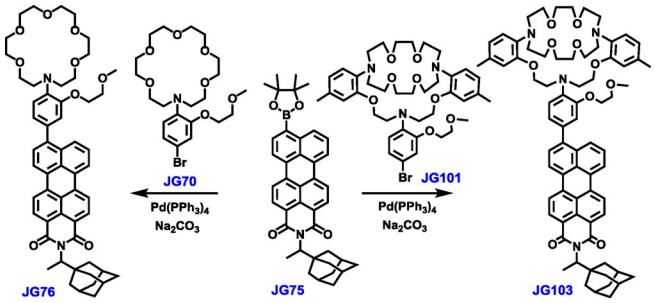

Scheme 1. Synthesis of JG76 and JG103.

With the simpler and more accessible JG76 fluorescent probe, we designed the fluorescence displacement assays on the basis of Figure 2. The displacement assays were initially performed by using commercial valinomycin instead of less-available cereulide. In this way, the JG76 probe was weakly fluorescent in ethanol, but in the presence of a potassium chloride solution, a dramatic increase in the fluorescence was observed owing to potassium-ion complexation. As expected, by the addition of a valinomycin solution, the previous solution became weakly fluorescent. The differences in fluorescence are described in Figure 2b.

On the other hand, probe JG103 showed very low solubility in ethanol and a very small increase in the fluorescence in the presence of potassium cations in all of the tested solvents; therefore, we considered that its utility for the detection of cereulide was very limited and its study was discontinued. Potassium cations are usually mixed with other ions in biological samples, so we checked carefully the action of diverse cations and anions that could interfere in the displacement assays with JG76. With respect to alkali-metal and alkaline-earth metal cations, the JG76 probe showed a large increase in fluorescence in the presence of potassium cations with total selectivity with respect to commonly found physiological cations (i.e. Li^+, Na^+, Mg^{2+}, Ca^{2+}, and NH_4^+) as well as less-common, albeit physiological cations (i.e. Sr^{2+}, Rb^+, Cs^+) but also showed a large increase in fluorescence in the presence of the highly toxic Be^{2+} and Ba^{2+} cations, which are not normally found in biological fluids (Figure 3) except in toxicological assays, for which the JG76 probe could be of interest.

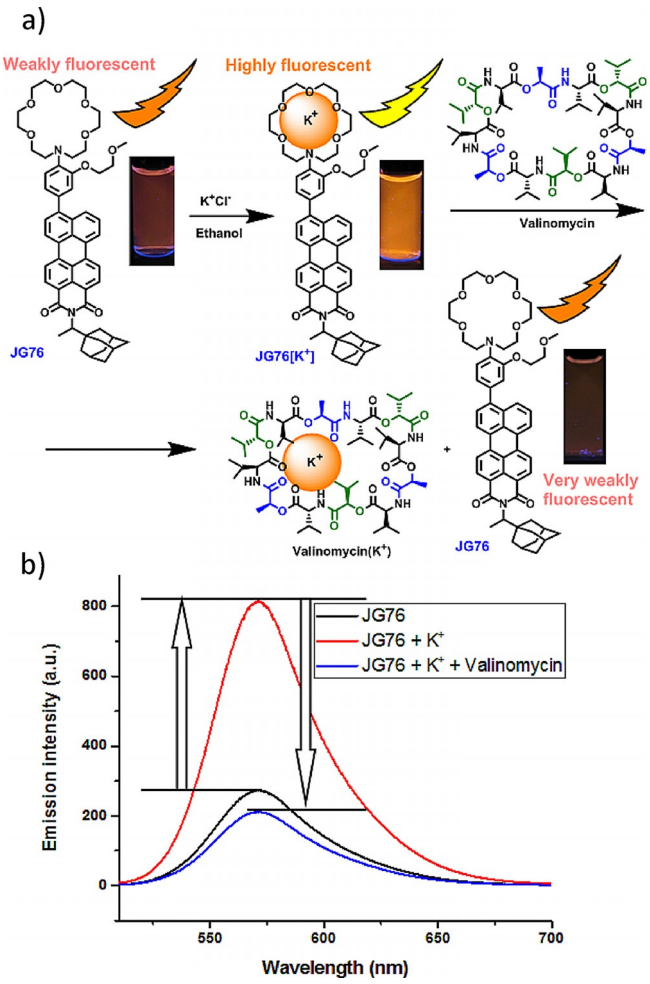

Figure 2. a) Qualitative and b) quantitative fluorescence displacement assays of JG76, potassium cations, and valinomycin.

The assays were performed by dissolving compound JG76 in EtOH to a concentration of 50 μM and the cations in water to a concentration of 5 mM; then, the cation solution (10 μL) was added to the JG76 solution (0.5 mL), and changes in the color and fluorescence were studied. With respect to heavy-metal cations, some acidic cations such as Sn^{2+} and Pb^{2+} showed a high increase in fluorescence in the presence of JG76, and to a lesser extent, some other cations, including Zn^{2+}, Cu^{2+}, Fe^{3+},

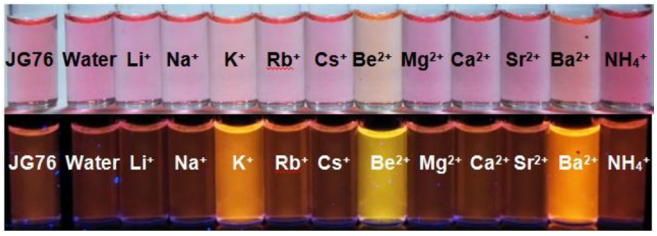

Figure 3. Color and fluorescence assays of JG76 and alkali-metal and alkaline-earth metal cations (1 equiv).

Sc^{3+}, Al^{3+}, Hg^{2+}, Au^{3+}, and Pd^{2+}, also showed an increase in fluorescence under the same conditions (Figure 4) and in the presence of a large excess amount of strong acids (pH < 5) or oxidants. None of the common anions [i.e. F^-, Cl^-, Br^-, I^-, BzO^- (Bz = benzoyl), NO_3^-, $H_2PO_4^-$, HSO_4^-, AcO^-, CN^-, SCN^-] gave a significant change in color or fluorescence (see the Supporting Information, Figure S98).

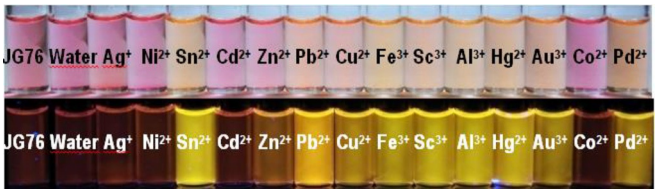

Figure 4. Color and fluorescence assays of JG76 and selected heavy-metal cations (1 equiv).

In a pH 7 buffered solution [JG76, 25 μM in EtOH/H_2O (7:3 v/v), 20 mM 4-(2-hydroxyethyl)-1-piperazineethanesulfonic acid (HEPES)], most of the interferent cations including Fe^{3+}, Sn^{2+}, Be^{2+}, and Cu^{2+} (5 equiv) did not promote a change in the fluorescence of JG76, but the sensitivity to K^+, Ba^{2+}, and Pb^{2+} remained unchanged, and they showed a high increase in the fluorescence of JG76; therefore, the only real interferents were the nonphysiological Ba^{2+} and Pb^{2+} cations (Figure 5).

Job's plot analysis, by representing $X_{JG76}(F_o-F)$ versus X_{JG76} (where X_{JG76} = mole fraction of JG76), afforded the stoichiometry of the complex, from the maximum position at $X_{JG76} = 0.5$, as a 1:1 complex. The calculated quantum yield of the JG76 probe in ethanol is Φ[JG76] (EtOH) = 0.04 ± 0.01 and for the corresponding potassium complex, Φ[JG76–K^+] (EtOH) = 0.17 ± 0.01; the increase is $\Phi/\Phi_0 = 4$, which is sufficient for the experimental assays. The lifetime of JG76 in EtOH was found to be 3.6 ns, and there was no change in the lifetime for the potassium complex. The limit of detection for K^+, obtained by linear regression of a titration of a 5 μM solution of JG76 in EtOH and K^+ by increasing the K^+ concentration from 0.01 to 0.2 μM and by measuring the increase in the fluorescence emission, was calculated as 0.06 μM, with a probability of false positive and false negative lower than 5%. The JG76–K^+ complex was studied by preparing a 2 μM solution of $K(CF_3SO_3)$ in EtOH and by increasing the concentration of JG76 from 0 to 10 μM without changing the concentration of K^+ in solution. The equilibrium constant (K) of the JG76–K^+ complex was calculated by fitting the fluorescence titration plot in ethanol by nonlinear least-square regression; the results were compared by performing first the titration of K^+ with JG76 and then that of JG76 with K^+, and the same results were obtained. The fitting calculation of the complexation constants was repeated three times to give $\log K$ (JG76 + K^+) = 6.34 ± 0.04. To validate the results, Job's plot analysis and the equilibrium constant of the JG76–K^+ complex were also studied and calculated in benzyl alcohol, BnOH, and comparable results were obtained: a 1:1 complex and $\log K$ (JG76–K^+) = 6.11 ± 0.03 (Figure 6). We next checked the suitability of the system for the practical detection of valinomycin by calculating the limit of detection of valinomycin in ethanol. Therefore, 0.75 equivalents of K^+ $CF_3SO_3^-$ was added to a 5 μM solution of JG76 in ethanol. Then, the concentration of valinomycin was increased by successive additions, and the fluorescence spectrum was registered. Regression of the titration plot of 5 μM JG76 and 3.75 μM K^+ in EtOH with valinomycin by decreasing the fluorescence emission gave a detection limit of 0.54 μM, with

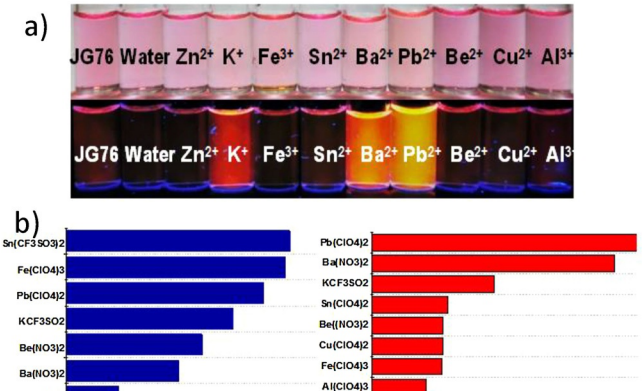

Figure 5. a) Color and fluorescence assays of JG76 and selected cations in a buffered pH 7 solution. b) Quantitative fluorescence assays of JG76 and selected cations in ethanol (left) and a buffered pH 7 solution (right).

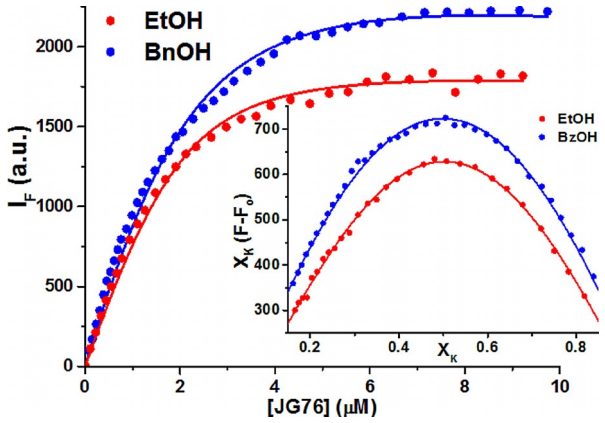

Figure 6. Fitted titration plot of a 2 μM solution of K^+ and JG76 by fluorescence emission in EtOH and BnOH. Inset: Job's plot of JG76 and K^+ by fluorescence emission in EtOH and BnOH.

a probability of false positive and false negative lower than 5% (see Figure S123).

The JG76 fluorescent probe was then ready for titration with synthetic cereulide, which was prepared according to the procedure of Biesta-Peters et al.[15] The last step, consisting of the cyclization of the linear H-(L-Val-D-*O*-Leu-D-Ala-L-*O*-Val-L-Val-D-*O*-Leu-D-Ala-L-*O*-Val-L-Val-D-*O*-Leu-D-Ala-L-*O*-Val)-OH depsipeptide, is shown in Scheme 2.

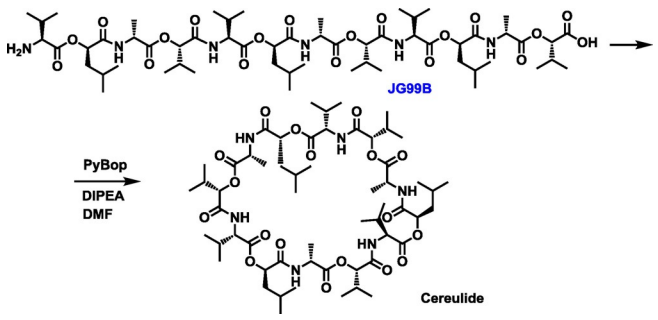

Scheme 2. Cereulide synthesis.

Purified cereulide was checked by NMR spectroscopy and HRMS (MALDI), and the results were identical to the reported data of cereulide. We first checked the suitability of the system for the practical detection of synthetic cereulide by calculating the limit of detection of cereulide in ethanol. In an experiment similar to that previously explained, $K^+CF_3SO_3^-$ (0.75 equiv) was added to a 5 μM solution of JG76 in ethanol. Then, the concentration of cereulide was increased by successive additions, and the fluorescence spectrum was registered. Regression of the titration plot of 5 μM JG76 and 3.75 μM K^+ in EtOH with cereulide by decreasing the fluorescence emission gave a detection limit of 0.21 μM, with a probability of false positive and false negative lower than 5% (Figure 7); in this case, the detection limit for cereulide was lower than the value obtained for valinomycin.

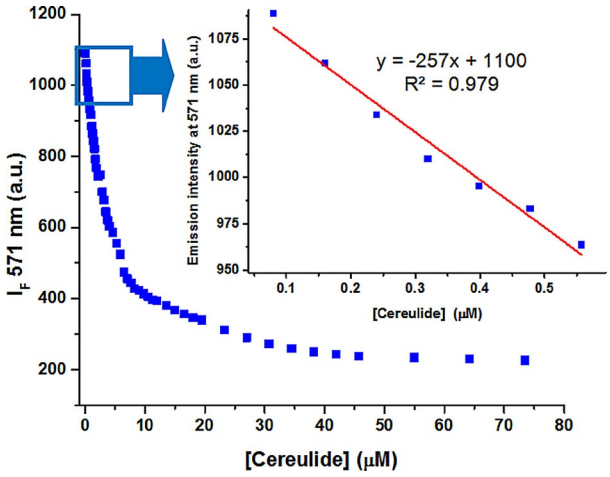

Figure 7. Linear regression of the titration plot of 5 μM JG76 and 3.75 μM K^+ in EtOH with increasing amounts of cereulide by decreasing the fluorescence emission of the system.

A complete description of the system was then performed by calculating the equilibrium constants between valinomycin/cereulide and the potassium cations in competitive equilibria with JG76, for which we previously obtained the binding constants. Equilibrium constants were first measured in EtOH solution by increasing the concentration of the probe in the presence of the analyte. We performed titrations of constant concentrations of 2 μM K^+ and 20 μM valinomycin or cereulide with JG76 (0 to 20 μM). In the case of valinomycin, the experiment started with solutions of valinomycin (V) and potassium cations (K) in ethanol so that the complex (VK) was produced in the equilibrium. Upon adding the JG76 probe (abbreviated S), it formed a complex with free K^+ and created a new complex (SK) and replaced the previous complex (VK). In this way, the concentration of VK decreased, whereas the concentration of V increased. The fluorescence intensity only depended on JG76 and the JG76–potassium complex. To solve the equations corresponding to the system, a possible approximation could be done, $C_V - [VK] \approx C_V$, in which C_V is the concentration of valinomycin, and this simplification is more realistic if the initial ratio of V/K is as high as possible. In this way, an equation to describe the equilibria was obtained [Eqs. (1)–(5)]:

$$S + K \overset{K_1}{\rightleftharpoons} SK \quad (1)$$

$$V + K \overset{K_2}{\rightleftharpoons} VK \quad (2)$$

$$K_1 = \frac{[SK]}{[S][K]} = \frac{[SK]}{(C_S - [SK])(C_K - [SK] - [VK])} \quad (3)$$

$$K_2 = \frac{[VK]}{[V][K]} = \frac{[VK]}{(C_V - [VK])(C_K - [SK] - [VK])} \quad (4)$$

$$[SK] = \frac{\left(C_S + C_K + \frac{1+K_2C_V}{K_1}\right) - \sqrt{\left(C_S + C_K + \frac{1+K_2C_V}{K_1}\right)^2 - 4C_SC_K}}{2} \quad (5)$$

in which C_S, C_K, and C_V are the concentrations of JG76, K^+, and valinomycin, respectively.

By taking into account the mass and fluorescence balances for all equilibria and performing the tests several times with different initial ratios of V/K (1:1, 1:0.25, and 1:0.1), the best fitting of the obtained equation was found at a 1:0.1 ratio, at which the approximation was most valid. By alternating the concentrations of valinomycin and cereulide in several experiments, fitted titration plots were obtained for both valinomycin and cereulide in EtOH and BnOH (Figure 8).

From the average of the three titrations, we obtained the following complexation equilibrium constants: $\log K$ (valinomycin–K^+, EtOH) = 5.97 ± 0.01, $\log K$ (valinomycin–K^+, BnOH) = 4.98 ± 0.01, $\log K$ (cereulide–K^+, EtOH) = 5.99 ± 0.01, K (cereulide–K^+, BnOH) = 5.01 ± 0.01. With the values of K_2 and K_1, the concentration of $[SK]_{eq}$ could be determined, and with these data the concentration of the species was calculated by using Equations (6)–(9). With the data previously obtained, the amounts of reagents and the proportion of the complex existing during the titration could be represented (Figure 9).

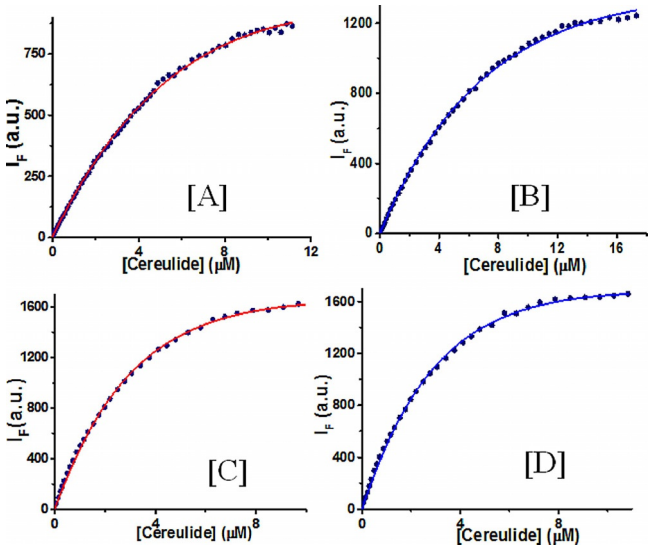

Figure 8. Fitted titration plots by fluorescence emission of 2 μM solutions of $K(CF_3SO_3)$ and a 20 μM solution of valinomycin or cereulide with JG76 in EtOH and BnOH: a) K^+, valinomycin, and JG76 in EtOH; b) K^+, valinomycin, and JG76 in BnOH; c) K^+, cereulide, and JG76 in EtOH; d) K^+, cereulide, and JG76 in BnOH.

$$[S]_{eq} = C_S - [SK]_{eq} \quad (6)$$

$$[VK]_{eq} = \frac{C_V + C_K - [SK]_{eq} + \frac{1}{K_2} \sqrt{\left(C_V + C_K - [SK]_{eq} + \frac{1}{K_2}\right)^2 - 4C_V(C_K - [SK]_{eq})}}{2} \quad (7)$$

$$[V]_{eq} = C_V - [VK]_{eq} \quad (8)$$

$$[K]_{eq} = C_K - [SK]_{eq} - [VK]_{eq} \quad (9)$$

To validate the method, we calculated the binding constant of valinomycin with potassium cations by circular dichroism following the reported methodology.[16] Starting with a concentration of 30 mM of valinomycin in EtOH, the concentration of the potassium cations was gradually increased up to 3.75 equivalents. This concentration of valinomycin was selected because of the optimal concentration to follow changes in the dichroism signal, albeit it is too high to perform safe measurements with toxic cereulide. By checking the fitting at different wavelengths, the value of the constant appeared to be different depending on the value of the wavelength selected. Within the $\lambda = 230$–250 nm range (at $\lambda = 238$ nm the obtained $\log K = 5.82$ value was similar to that previously reported), the calculated range of values for the complexation constant was $\log K$(valinomycin–K^+, EtOH) = 5.8–6.0, which is compatible with the values obtained by fluorescence assays. Therefore, the developed methodology was validated as a means to study the fluorescence detection of cereulide from natural samples. To accomplish this objective, the proposed method involved the competition between cereulide and the JG76 probe for potassium. Extraction of natural cereulide was performed on cultures of *B. cereus* F4810/72 by following the methodology de-

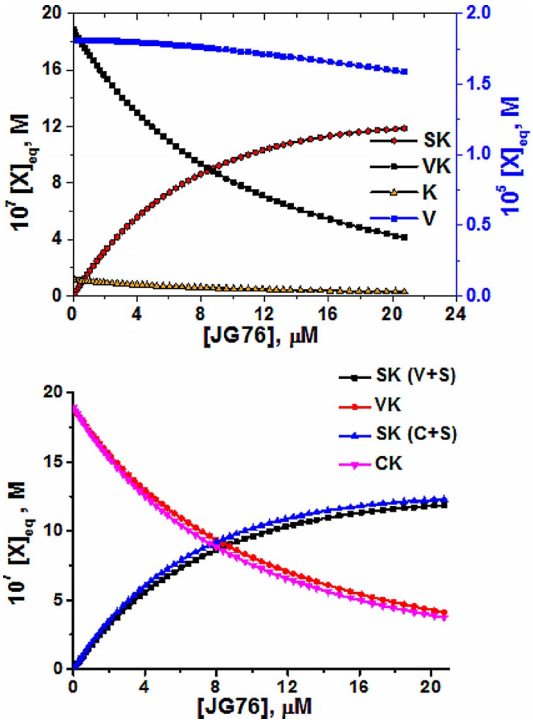

Figure 9. Concentrations in equilibrium in EtOH solution. Top) V (valinomycin), VK (valinomycin–K^+), K (K^+), and SK (JG76–K^+) in equilibrium. Bottom) comparison of the concentrations of the complexes corresponding to valinomycin and cereulide and CK (cereulide–K^+) in equilibrium.

veloped for cooked rice,[17] which consisted of inoculation of rice with 300 Cfu (average value found in rice dishes). Cfu was determined at several time points, and cereulide production was checked at several time points by MS (UPLC-TOF). We measured the change in fluorescence in the presence of a constant concentration of the probe, a constant concentration of potassium, and an unknown concentration of the cereulide sample (usually within the range of 0.2 to 3.5 μM in acetonitrile), which we titrated with synthetic cereulide. Initial acetonitrile extracts were evaporated, the residue was extracted into dichloromethane/water and concentrated, and the obtained solid was dissolved in EtOH so that the interference of water-soluble interferents was prevented. The EtOH solution was checked by MS (UPLC-TOF) by studying the elution time of synthetic cereulide, and the LC–MS of the extracted cereulide samples were measured and calibrated with synthetic cereulide at different concentrations. In this way, the concentration of the cereulide samples from rice remained between 1.2 and 1.6 μM [as determined by MS (UPLC)]. We then measured the background fluorescence due to the matrix of the sample. We performed a preliminary titration of the sample with JG76 to assure that the background fluorescence was a constant value independent of the amount of JG76 (Figure 10).

With the extracted cereulide samples we measured variations in the emission signal by subtracting the background fluorescence of the matrix, measured before adding JG76, and titrated the samples with synthetic cereulide in the presence of JG76 (2 μM) and K^+ (0.75 μM). With this titration we ob-

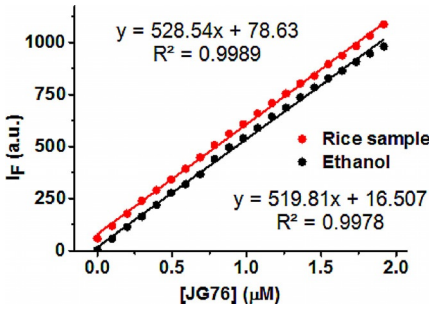

Figure 10. Comparison between ethanol and rice sample solutions upon increasing the JG76 concentration. The background fluorescence was a constant value of 77 au.

served that the first points of the rice sample titration deviated from those of the reference due to the quantity of natural cereulide present in the sample; therefore, from the initial values of fluorescence we obtained the original concentration of natural cereulide in the sample by comparison with the reference plot from synthetic cereulide (Figure 11). The result of repeating the test three times was (1.0±0.2) μM for rice samples compared to the concentration of 1.2 μM obtained by mass spectrometry. In the case of a sample spiked with 1.75 μM cereulide, the result of the fluorescence titration was in accordance with the expected value (Figure 12). If there was no initial cereulide in the sample, the curves were coincident (Figure 13).

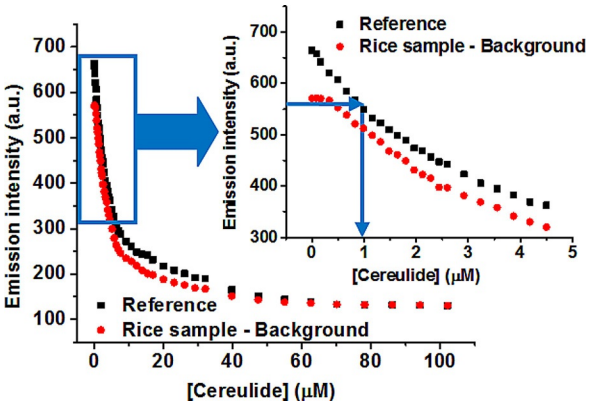

Figure 11. Fluorescence emission of a corrected sample versus the reference by titration with increasing quantities of cereulide. The concentration of JG76 was 2 μM, and the concentration of K^+ was 0.75 μM. The concentration of cereulide in the rice sample was 0.95 μM.

Indeed, the measurements were more precise for the samples spiked with synthetic cereulide than for the samples containing natural cereulide, which is due to the fact that natural samples have more than one type of cereulide.[18] The existence of a mixture of natural cereulides (isocereulides) introduces some uncertainty in the experimental measurements, because their potassium-ion-complexation constants are not known. The fluorescence detection of natural cereulide in rice samples by using synthetic cereulide and a potassium fluorescent reporter is therefore a useful, portable, and fast method

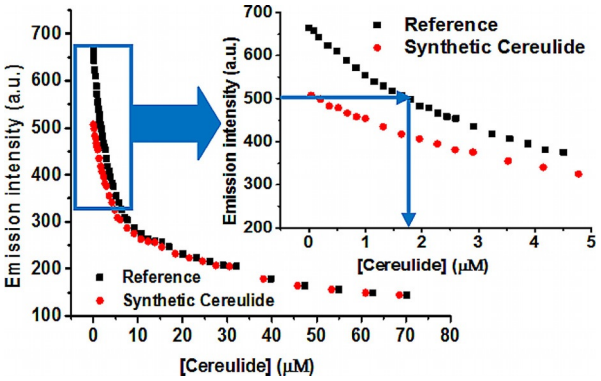

Figure 12. Fluorescence emission of a rice sample spiked with 1.75 μM cereulide versus the reference by titration with increasing quantities of cereulide. The concentration of JG76 was 2 μM, and the concentration of K^+ was 0.75 μM.

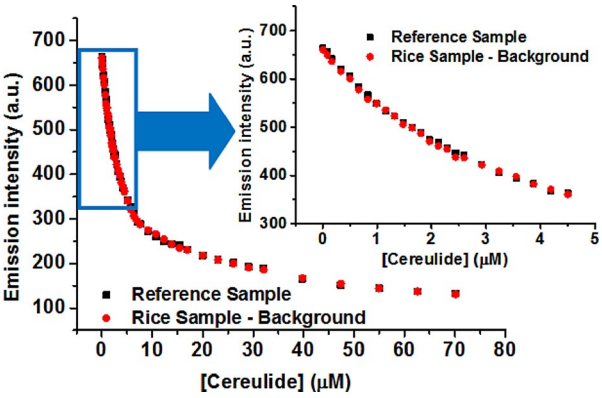

Figure 13. Fluorescence emission of a rice sample with no cereulide versus the reference by titration with increasing quantities of cereulide. The concentration of JG76 was 2 μM, and the concentration of K^+ was 0.75 μM.

for the in situ detection of cereulide by simple extraction and fluorescence titration of the sample. In the case of positive detection, the method can be complemented by standard methodology involving LC–MS for more accurate analysis. Taking into account that a LC–MS (Q-TOF) instrument is not a cheap or portable device relative to a benchtop fluorometer, the reported method may easily prevent the occurrence of foodborne outbreaks by emetic toxin by in situ detection of cereulide.

Another interesting aspect of cereulide detection is visualization of the action of cereulide in live cells. For this purpose, we performed cellular localization studies in HeLa cells (human cervical carcinoma cells) with the JG76 fluorogenic probe. HeLa cells, cultured under standard conditions,[19] were incubated with the probe (18 μM in 1% v/v DMSO/culture medium). Cells were fixed with 4% paraformaldehyde before taking images. The nuclei of the fixed cells were stained with Hoechst dye (bisbenzimide) before high-resolution confocal microscopy imaging was performed. All confocal cell images were pseudocolored (Figure 14). After exposure for 12 h, the probe stained intracellular vesicular structures that resembled endolysosomes (Figure 14, top). After exposure for 24 h, the

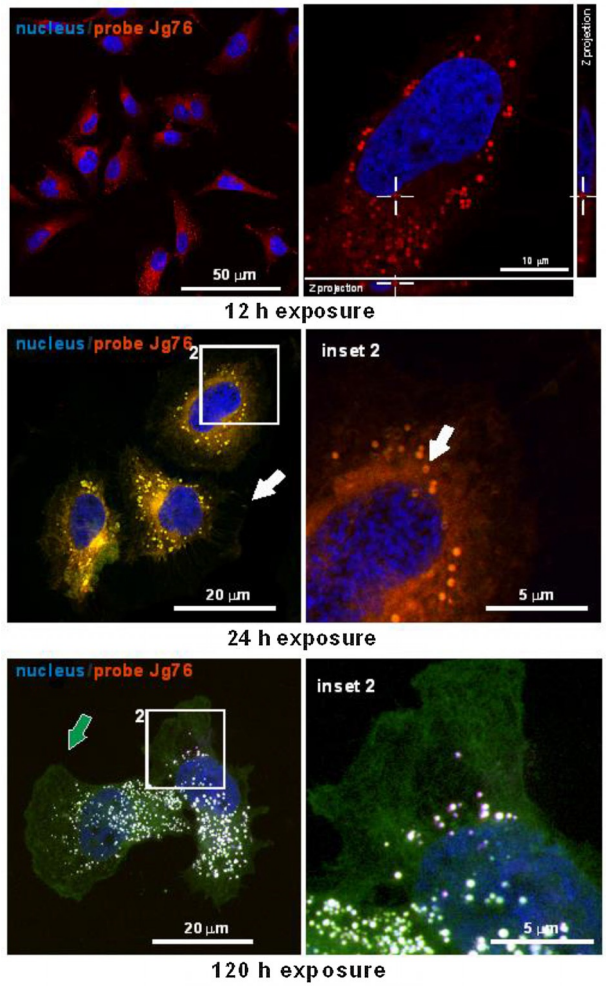

Figure 14. Top) Confocal microscopy projection images of the JG76 probe in HeLa cells 12 h after staining; right) *Z*-lateral projection images of the locations of the stained structures inside fixed HeLa cells 12 h after staining. Nuclei are stained with Hoechst dye (blue channel). Middle) Confocal microscopy projection images of the JG76 probe in HeLa cells 24 h after staining obtained by exciting the probe sequentially with $\lambda = 488$, 562, and 638 nm lasers. Different fluorophore emissions are pseudocolored in their respective wavelengths (green: 500–550 nm; red: 570–620 nm, purple: 662–737 nm). Bottom) Confocal microscopy projection images of the JG76 probe in HeLa cells 120 h after staining.

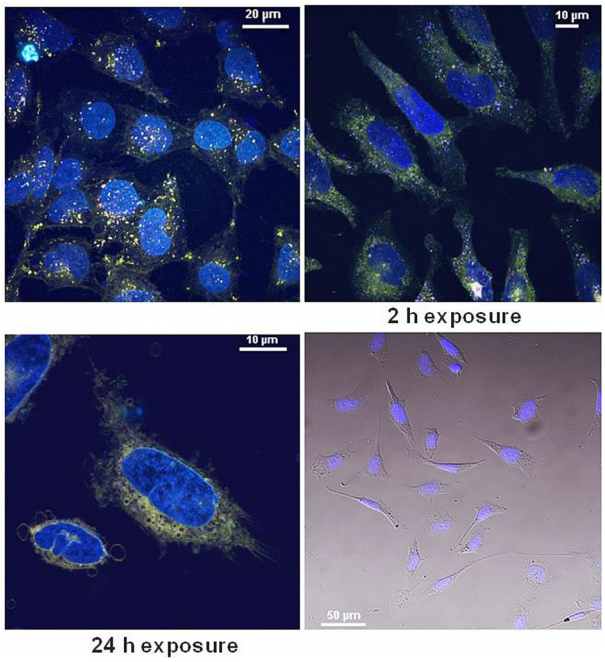

Figure 15. Top left) Confocal microscopy projection images of the JG76 probe in HeLa cells 2 h after staining obtained by exciting the probe sequentially with a $\lambda = 488$ nm laser. Nuclei are stained with Hoechst dye (blue channel). Top right) Confocal microscopy projection images of the JG76 probe in HeLa cells 2 h after the addition of cereulide to the previous sample. Bottom left) Confocal microscopy projection image of the JG76 probe in HeLa cells 24 h after the addition of cereulide to the first sample showing large dark vacuoles. Bottom right) Fluorescence microscopy image of HeLa cells 12 h after the addition of cereulide, used as a reference. Nuclei are stained with Hoechst dye (blue channel).

JG76 probe displayed an endosomal-RER pattern clearly localized within the cytoplasmic and endosomal membranes (arrows) (Figure 14, middle). After 120 h of staining, the JG76 probe was also localized in the cytoplasmic membrane (green arrow) (Figure 14, bottom). HeLa cells did not display detectable signs of toxicity if grown in the presence of the potassium-ion JG76 fluorescent probe for up to 120 h.

Then, HeLa cells, cultured under standard conditions, were incubated with the probe (0.1 mg mL^{-1}) for 2 h. Samples of cells were fixed with 4% paraformaldehyde before images were taken. The nuclei of the fixed cells were stained with Hoechst dye (bisbenzimide) before high-resolution confocal microscopy imaging was performed. All confocal cell images were pseudocolored (excitation at $\lambda = 488$ nm and emission in the green/red/near-red region) (Figure 15). Similar to the previous experiment, the probe stained intracellular vesicular structures (Figure 15, top left). After exposure to JG76 for 2 h, the cells were exposed to synthetic cereulide (0.2 mg mL^{-1}) for another 2 h (Figure 15, top right). After exposure to JG76 and cereulide for 2 h, the near-red emission of the endosomes was diminished (more pink, less green in pseudocolor), and the staining of the cytoplasmic membrane also diminished. The cytosol appeared to be more stained with the probe. At 24 h after the addition of cereulide to the cells exposed to JG76, the cellular viability decreased significantly and several cells appeared wrinkled and showed membrane blebbing and cytosol vacuolization.

From the images it is clear that the initial fluorescence of JG76, complexed with potassium ions in the potassium-rich structures of the cells, is quenched by cereulide in HeLa cells through potassium-ion-displacement complexation, and this leaves only the residual fluorescence of JG76 in the membranes of the cells as evidence for the action of cereulide. Even more, morphological changes in the HeLa cells, such as the formation of large vacuoles and membrane blebbing, as a result of the action of cereulide with time are easily followed by the residual fluorescence of JG76 on the membranes; this proves the efficiency of the JG76 probe as a cereulide chemical sensor by potassium-ion-complexation displacement. Therefore, the JG76 fluorescent probe can be considered as a useful tool for the visualization of cereulide in live cells and for the lo-

calization of highly polar potassium-rich structures, in comparison to low-polarity membrane structures, from live cells.

3. Conclusions

In conclusion, we developed a fluorogenic procedure that was able to detect cereulide, a toxic metabolite produced by specific strains of *Bacillus cereus*, in rice samples through displacement of potassium cations from a preformed specific complex with a subsequent change in the fluorescence emission. The designed fluorescent probe for potassium cations was suitable for displacement assays with cereulide from organic extracts so that the fluorescence detection of natural cereulide in rice samples was achieved, and this was proven to be a portable and fast method for the in situ detection of cereulide in food extracts. To study the fate of cereulide in live cells, we designed a procedure suitable for live-cell microscopy imaging of HeLa cells by comparing the cellular location of the potassium fluorogenic probe, which stained intracellular vesicular structures that resembled endolysosomes, in the absence and presence of cereulide. We were able to conclude that in the presence of cereulide the fluorescence of the probe was decreased because of complexation of the potassium ions by cereulide.

Experimental Section

Synthesis of JG76

$Pd(PPh_3)_4$ (10 mg, 5 mol%) was added to a solution of 16-[4-bromo-2-(2-methoxyethoxy)phenyl]-1,4,7,10,13-pentaoxa-16-azacyclooctadecane (JG70; 100 mg, 0.16 mmol) in toluene/*n*BuOH (15 mL/4 mL) under a nitrogen atmosphere in a 100 mL Schlenk flask. Then, a solution of *N*-[1-(1-adamantyl)ethyl]-8-pinacolylboronateperylene-3,4-dicarboxylmonoimide (JG75; 81 mg, 0.16 mmol) in toluene/*n*BuOH/water (5 mL:1.5 mL:0.5 mL) was added, followed by Na_2CO_3 (174 mg, 1.64 mmol), and the mixture was heated under reflux for 24 h. The mixture was then poured into water (100 mL), extracted with CH_2Cl_2 (3×100 mL), and worked-up, and then the residue was purified by column chromatography (silica gel, CH_2Cl_2/MeOH 92:8 v/v) to give *N*-[1-(1-adamantyl)ethyl]-8-[4-(1,4,7,10,13-pentaoxa-16-azacyclooctadecan-16-yl)-3-(2-methoxyethoxy)phenyl]perylene-3,4-dicarboxylmonoimide (JG76; 58 mg, 40%) as a purple solid. M.p. 135–136 °C. ^{1}H NMR (300 MHz, $CDCl_3$): δ = 8.53 (m, 2H, $C_{Ar}H$), 8.49–8.33 (m, 3H, $C_{Ar}H$), 8.02 (m, 1H, $C_{Ar}H$), 7.59–7.54 (m, 2H, $C_{Ar}H$), 7.25–6.91 (m, 4H, $C_{Ar}H$), 5.10 (q, J = 7.1 Hz, 1H, CH), 4.23 (m, 2H, CH_2), 3.80–3.54 (m, 24H, 12CH_2), 3.66–3.40 (s, 5H, CH_2 + CH_3), 1.98 (m, 3H, 3CH), 1.85–1.81 (m, 3H, 1.5CH_2), 1.73–1.62 ppm (m, 12H, 4.5CH_2 + CH_3). ^{13}C NMR (100 MHz, $CDCl_3$): δ = 173.7 (C=O), 165.7 (C_{Ar}), 165.0 (C_{Ar}), 136.8 (C_{Ar}), 132.6–123.2 (C_{Ar} + CH_{Ar}), 121.9 (C_{Ar}), 121.0 (C_{Ar}), 120.1 ($C_{Ar}H$), 116.5 (C_{Ar}), 72.1–67.0 (CH_2), 59.3–58.2 (CH + CH_3), 40.5 (CH), 38.9 (CH_2), 38.2 (C_q), 37.2 (CH), 34.2 (CH), 32.1–29.5 ppm (CH + CH_3). IR (KBr): $\tilde{\nu}$ = 2955, 2924, 2848, 1738 (C=O), 1692 (C=O), 1685 (C=O), 1651, 1590, 1571, 1506, 1457, 1384, 1354, 1248, 1122 cm^{-1}. HRMS (MALDI): *m/z*: calcd for $C_{55}H_{63}N_2O_9$: 895.4528 $[M+H]^+$; found: 895.4535.

Synthesis of Triazacryptand-perylenemonoimide JG103

$Pd(PPh)_3$ (5.6 mg, 5 mol%) was added to a solution of bromotriazacryptand JG101 (59 mg, 0.097 mmol) dissolved in toluene/*n*BuOH (10 mL:3.3 mL) under a nitrogen atmosphere in a 100 mL Schlenk flask. Then, boronic ester JG75 (82 mg, 0.10 mmol) dissolved in toluene/*n*BuOH (3.5 mL:1 mL) was added dropwise. Then, Na_2CO_3 (102.2 mg, 0.97 mmol) dissolved in water (3 mL) was added, and the mixture was stirred under reflux for 24 h. The mixture was poured into water (30 mL), and the product was extracted with CH_2Cl_2 (3×100 mL). After workup, the solid residue was purified by column chromatography (silica gel, CH_2Cl_2/MeOH 50:4) from which the triazacryptand-perylenemonoimide JG103 (48 mg, 42%) was obtained as a purple solid. M.p. 193–195 °C. ^{1}H NMR (300 MHz, $CDCl_3$): δ = 8.53 (m, 2H, $C_{Ar}H$), 8.49–8.33 (m, 3H, $C_{Ar}H$), 8.02 (m, 1H, $C_{Ar}H$), 7.59–7.54 (m, 2H, $C_{Ar}H$), 7.25–6.91 (m, 4H, $C_{Ar}H$), 5.10 (q, J = 7.1 Hz, 1H, CH), 4.23–3.50 (m, 39H, 18CH_2 + CH_3), 2.26–2.20 (m, 6H, 2CH_3), 1.98 (m, 3H, 3CH), 1.85–1.81 (m, 2H, CH_2), 1.73–1.62 ppm (m, 13H, 6CH_2 + CH_3). ^{13}C NMR (100 MHz, $CDCl_3$): δ = 165.8 (C_{Ar}), 165.1 (C_{Ar}), 153.2 (C_{Ar}), 137.3 (C_{Ar}), 132.9, 132.3, 132.2, 130.0, 129.6, 128.9, 128.5, 128.2, 127.0, 126.8, 126.7, 123.5, 122.3, 121.3, 120.4, 120.1, 114,8, 114.4, 114.2, and 110.0 (C_{Ar} + CH_{Ar}), 71.4, 71.0, 70.8, 70.5, 69.6, 68.2, and 67.3 (CH_2), 59.2 (CH_3), 58.2 (CH), 53.6–52.5 (CH_2), 40.4 (CH), 38.2 (C_q), 37.1 (CH), 31.7, 31.1, 29.2, and 29.0 (CH + CH_2), 21.3 (CH_2), 14.3 and 13.3 ppm (CH_3). IR (KBr): $\tilde{\nu}$ = 2955, 2922, 2856, 1736 (C=O), 1696 and 1682 (C=O), 1651, 1592, 1557, 1509, 1456, 1351, 1250, 1170, 1119, 1106, 1049, 959, 812, 750, 721, 697, 667 cm^{-1}. HRMS (ESI): *m/z*: calcd for $C_{73}H_{82}N_4NaO_{10}$: 1197.5923 $[M+Na]^+$; found: 1197.6001.

Acknowledgements

We gratefully acknowledge financial support from the Ministerio de Economía y Competitividad, Spain (Projects CTQ2015-71353-R and AES-PI16/000496), Junta de Castilla y León, Consejería de Educación y Cultura y Fondo Social Europeo (Project BU232U13), and the European Commission, Seventh Framework Programme (Project SNIFFER FP7-SEC-2012–312411). J. G.-C. thanks Ministerio de Economía y Competitividad for his predoctoral FPU fellowship.

Conflict of Interest

The authors declare no conflict of interest.

Keywords: cereulide · fluorescent probes · potassium · sensors · valinomycin

[1] a) L. P. Stenfors Arnesen, A. Fagerlund, P. E. Granum, *FEMS Microbiol. Rev.* **2008**, *32*, 579–606; b) E. Granum, T. Lund, *FEMS Microbiol. Lett.* **1997**, *157*, 223–228.
[2] G. Lücking, M. K. Dommel, S. Scherer, A. Fouet, M. Ehling-Schulz, *Microbiology* **2009**, *155*, 922–931.
[3] S. Ceuppens, N. Boon, M. Uyttendaele, *FEMS Microbiol. Ecol.* **2013**, *84*, 433–450.
[4] M. Kranzler, K. Stollewerk, K. Rouzeau-Szynalski, L. Blayo, M. Sulyok, M. Ehling-Schulz, *Front. Microbiol.* **2016**, *7*, 1640, https://doi.org/10.3389/fmicb.2016.01640.
[5] Y. Cui, Y. Liu, X. Liu, X. Xia, S. Ding, K. Zhu, *Toxins* **2016**, *8*, 156, https://doi.org/10.3390/toxins8060156.
[6] N. A. Logan, *J. Appl. Microbiol.* **2011**, *112*, 417–429.
[7] a) N. A. Magarvey, M. Ehling-Schulz, C. T. Walsh, *J. Am. Chem. Soc.* **2006**, *128*, 10698–10699; b) M. Ehling-Schulz, E. Frenzel, M. Gohar, *Front. Microbiol.* **2015**, *6*, 704, https://doi.org/10.3389/fmicb.2015.00704; c) G. Lücking, E. Frenzel, A. Rütschle, S. Marxen, T. D. Stark, T. Hofmann, S.

Scherer, M. Ehling-Schulz, *Front. Microbiol.* **2015**, *6*, 1101, https://doi.org/10.3389/fmicb.2015.01101.

[8] Cereulide: a) A. Makarasen, K. Yoza, M. Isobe, *Chem. Asian J.* **2009**, *4*, 688–698; b) A. Makarasen, T. Nishikawa, M. Isobe, *Synthesis* **2009**, 2184–2204; valinomycin: c) C. Annese, D. I. Abbrescia, L. Catucci, L. D'Accolti, N. Denora, I. Fanizza, C. Fusco, G. La Piana, *J. Pept. Sci.* **2013**, *19*, 751–757; d) R. M. Iacobazzi, C. Annese, A. Azzariti, L. D'Accolti, M. Franco, C. Fusco, G. La Piana, V. Laquintana, N. Denora, *ACS Med. Chem. Lett.* **2013**, *4*, 1189–1192.

[9] a) M. M. Häggblom, C. Apetroaie, M. A. Andersson, M. S. Salkinoja-Salonen, *Appl. Environ. Microbiol.* **2002**, *68*, 2479–2483; b) T. Bauer, T. Stark, T. Hofmann, M. Ehling-Schulz, *J. Agric. Food Chem.* **2010**, *58*, 1420–1428; c) V. Fricker, U. Messelhaüßer, U. Busch, S. Scherer, M. Ehling-Schulz, *Appl. Environ. Microbiol.* **2007**, *73*, 1892–1898; d) H. T. Rønning, T. N. Asp, P. E. Granum, *Food Addit. Contam. A* **2015**, *32*, 911–921; e) L. Delbrassinne, M. Andjelkovic, A. Rajkovic, P. Dubois, E. Nguessan, J. Mahillon, J. Van Loco, *Food Anal. Methods* **2012**, *5*, 969–979.

[10] a) M. A. Andersson, P. Hakulinen, U. Honkalampi-Hamalainen, D. Hoornstra, J.-C. Lhuguenot, J. Maki-Paakkanen, M. Savolainen, I. Severin, A.-L. Stammati, L. Turco, A. Weber, A. von Wright, F. Zucco, M. Salkinoja-Salonen, *Toxicon* **2007**, *49*, 351–367; b) E. L. Jääskeläinen, V. Teplova, M. A. Andersson, L. C. Andersson, P. Tammela, M. C. Andersson, T. I. Pirhonen, N.-E. L. Saris, P. Vuorela, M. S. Salkinoja-Salonen, *Toxicol. in Vitro* **2003**, *17*, 737–744.

[11] a) J. García-Calvo, S. Vallejos, F. C. García, J. Rojo, J. M. García, T. Torroba, *Chem. Commun.* **2016**, *52*, 11915–11918; b) J. García-Calvo, P. Calvo-Gredilla, M. Ibañez-Llorente, T. Rodríguez, T. Torroba, *Chem. Rec.* **2016**, *16*, 810–824; c) B. Díaz de Greñu, J. García-Calvo, J. Cuevas, G. García-Herbosa, B. García, N. Busto, S. Ibeas, T. Torroba, B. Torroba, A. Herrera, S. Pons, *Chem. Sci.* **2015**, *6*, 3757–3764; d) B. Díaz de Greñu, D. Moreno, T. Torroba, A. Berg, J. Gunnars, T. Nilsson, R. Nyman, M. Persson, J. Pettersson, I. Eklind, P. Wästerby, *J. Am. Chem. Soc.* **2014**, *136*, 4125–4128.

[12] a) S. Kaloyanova, Y. Zagranyarski, S. Ritz, M. Hanulová, K. Koynov, A. Vonderheit, K. Müllen, K. Peneva, *J. Am. Chem. Soc.* **2016**, *138*, 2881–2884; b) U. Lewandowska, W. Zajaczkowski, L. Chen, F. Bouillière, D. Wang, K. Koynov, W. Pisula, K. Müllen, H. Wennemers, *Angew. Chem. Int. Ed.* **2014**, *53*, 12537–12541; *Angew. Chem.* **2014**, *126*, 12745–12749; c) A. Bolag, N. Sakai, S. Matile, *Chem. Eur. J.* **2016**, *22*, 9006–9014; d) J. A. Hutchison, H. Uji-i, A. Deres, T. Vosch, S. Rocha, S. Müller, A. A. Bastian, J. Enderlein, H. Nourouzi, C. Li, A. Herrmann, K. Müllen, F. De Schryver, J. Hofkens, *Nat. Nanotechnol.* **2014**, *9*, 131–136; e) U. Lewandowska, W. Zajaczkowski, W. Pisula, Y. Ma, C. Li, K. Müllen, H. Wennemers, *Chem. Eur. J.* **2016**, *22*, 3804–3809.

[13] a) T. Schwarze, R. Schneider, J. Riemer, H.-J. Holdt, *Chem. Asian J.* **2016**, *11*, 241–247; b) T. Schwarze, J. Riemer, S. Eidner, H.-J. Holdt, *Chem. Eur. J.* **2015**, *21*, 11306–11310; c) S. Ast, T. Schwarze, H. Müller, A. Sukhanov, S. Michaelis, J. Wegener, O. S. Wolfbeis, T. Körzdörfer, A. Dürkop, H.-J. Holdt, *Chem. Eur. J.* **2013**, *19*, 14911–14917.

[14] a) B. Sui, X. Yue, M. G. Tichy, T. Liu, K. D. Belfield, *Eur. J. Org. Chem.* **2015**, 1189–1192; b) H. He, M. A. Mortellaro, M. J. P. Leiner, R. J. Fraatz, J. K. Tusa, *J. Am. Chem. Soc.* **2003**, *125*, 1468–1469; see also: c) X. Zhou, F. Su, Y. Tian, C. Youngbull, R. H. Johnson, D. R. Meldrum, *J. Am. Chem. Soc.* **2011**, *133*, 18530–18533; d) W. Namkung, P. Padmawar, A. D. Mills, A. S. Verkman, *J. Am. Chem. Soc.* **2008**, *130*, 7794–7795; e) X. Zhou, F. Su, W. Gao, Y. Tian, C. Youngbull, R. H. Johnson, D. R. Meldrum, *Biomaterials* **2011**, *32*, 8574–8583; f) R. D. Carpenter, A. S. Verkman, *Org. Lett.* **2010**, *12*, 1160–1163; g) X. Li, X. Gao, W. Shi, H. Ma, *Chem. Rev.* **2014**, *114*, 590–659; h) T. Hirata, T. Terai, H. Yamamura, M. Shimonishi, T. Komatsu, K. Hanaoka, T. Ueno, Y. Imaizumi, T. Nagano, Y. Urano, *Anal. Chem.* **2016**, *88*, 2693–2700.

[15] E. G. Biesta-Peters, M. W. Reij, R. H. Blaauw, P. H. in't Veld, A. Rajkovic, M. Ehling-Schulz, T. Abee, *Appl. Environ. Microbiol.* **2010**, *76*, 7466–7472.

[16] M. C. Rose, R. W. Henkens, *Biochim. Biophys. Acta Gen. Subj.* **1974**, *372*, 426–435.

[17] a) A. Zuberovic Muratovic, R. Tröger, K. Granelli, K.-E. Hellenäs, *Toxins* **2014**, *6*, 3326–3335; b) M. Yamaguchi, T. Kawai, M. Kitagawa, Y. Kumeda, *Food Microbiol.* **2013**, *34*, 29–37; c) M. Decleer, A. Rajkovic, B. Sas, A. Madder, S. De Saeger, *J. Chromatogr. A* **2016**, *1472*, 35–43.

[18] a) S. Marxen, T. D. Stark, E. Frenzel, A. Rütschle, G. Lücking, G. Pürstinger, E. E. Pohl, S. Scherer, M. Ehling-Schulz, T. Hofmann, *Anal. Bioanal. Chem.* **2015**, *407*, 2439–2453; b) S. Marxen, T. D. Stark, A. Rütschle, G. Lücking, E. Frenzel, S. Scherer, M. Ehling-Schulz, T. Hofmann, *Sci. Rep.* **2015**, *5*, 10637, https://doi.org/10.1038/srep10637; c) S. Marxen, T. D. Stark, A. Rütschle, G. Lücking, E. Frenzel, S. Scherer, M. Ehling-Schulz, T. Hofmann, *J. Agric. Food Chem.* **2015**, *63*, 8307–8313.

[19] a) L. Rodriguez-Fernandez, R. Valiente, J. Gonzalez, J. C. Villegas, M. L. Fanarraga, *ACS Nano* **2012**, *6*, 6614–6625; b) L. García-Hevia, R. Valiente, R. Martín-Rodríguez, C. Renero-Lecuna, J. González, L. Rodríguez-Fernández, F. Aguado, J. C. Villegasa, M. L. Fanarraga, *Nanoscale* **2016**, *8*, 10963–10973; c) B. Sanz, M. P. Calatayud, T. E. Torres, M. L. Fanarraga, M. R. Ibarra, G. F. Goya, *Biomaterials* **2017**, *114*, 62–70.

Received: March 21, 2017
Version of record online June 12, 2017

